Environmental Science & Technology

Article

pubs.acs.org/est

Molecular Characterization of Organosulfur Compounds in Biodiesel and Diesel Fuel Secondary Organic Aerosol

Sandra L. Blair,[†] Amanda C. MacMillan,[†] Greg T. Drozd,[‡] Allen H. Goldstein,[‡] Rosalie K. Chu,[§] Ljiljana Paša-Tolić,[§] Jared B. Shaw,[§] Nikola Tolić,[§] Peng Lin,[§] Julia Laskin,[∥] Alexander Laskin,[§] and Sergey A. Nizkorodov*[,†]

[†]Department of Chemistry, University of California, Irvine, Irvine, California 92697, United States

[‡]Department of Environmental Science, Policy, & Management, University of California, Berkeley, Berkeley, California 94720, United States

[§]Environmental Molecular Sciences Laboratory and [∥]Physical Sciences Division, Pacific Northwest National Laboratory, Richland, Washington 99354, United States

Supporting Information

ABSTRACT: Secondary organic aerosol (SOA), formed in the photooxidation of diesel fuel, biodiesel fuel, and 20% biodiesel fuel/80% diesel fuel mixture, are prepared under high-NO_x conditions in the presence and absence of sulfur dioxide (SO_2), ammonia (NH_3), and relative humidity (RH). The composition of condensed-phase organic compounds in SOA is measured using several complementary techniques including aerosol mass spectrometry (AMS), high-resolution nanospray desorption electrospray ionization mass spectrometry (nano-DESI/HRMS), and ultrahigh resolution and mass accuracy 21T Fourier transform ion cyclotron resonance mass spectrometry (21T FT-ICR MS). Results demonstrate that sulfuric acid and condensed organosulfur species formed in photooxidation experiments with SO_2 are present in the SOA particles. Fewer organosulfur species are formed in the high humidity experiments, performed at RH 90%, in comparison with experiments done under dry conditions. There is a strong overlap of organosulfur species observed in this study with previous field and chamber studies of SOA. Many MS peaks of organosulfates ($R-OS(O)_2OH$) previously designated as biogenic or of unknown origin in field studies might have originated from anthropogenic sources, such as photooxidation of hydrocarbons present in diesel and biodiesel fuel.

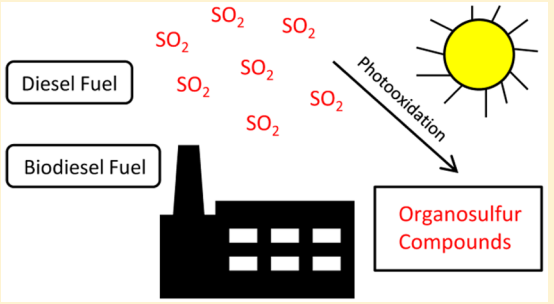

INTRODUCTION

Atmospheric aerosols contribute significantly to decreased visibility,[1] increased morbidity and premature mortality,[2] and uncertainty in climate predictions of atmospheric models.[3] In particular, organic aerosols (OA), which contain thousands of organic compounds,[4] are often the major component of aerosol particles, providing up to 90% of the submicrometer particle mass.[5] Primary organic aerosols (POA) are directly emitted into the atmosphere from sources such as vehicles, industrial processing, biomass burning, and sea spray. Oxidation of volatile organic compounds (VOCs) in the atmosphere form low vapor pressure oxidized organics that condense into secondary organic aerosols (SOA) which can amount to 50–85% of the overall contribution to OA.[6]

Urban atmospheric environments contain a highly complex mixture of both natural and anthropogenic primary and secondary air pollutants, including VOCs, POA, SOA, SO_2, NO_x, NH_3, etc. Traffic is the most important emission source of $PM_{2.5}$ (primary particulate matter with diameters ≤ 2.5 μm), accounting for up to one-third of $PM_{2.5}$ mass.[7] Diesel vehicle exhaust can contain a large contribution from unburned fuel, which releases reactive gas-phase hydrocarbons that act as a source of newly formed SOA.[8] Similarly, biodiesel fuel exhaust can also contain unburned fuel, such as fatty acid methyl esters (FAMEs).[9] Such products of incomplete combustion and incomplete catalyst oxidation may be efficient SOA precursors.[10] Other sources of fugitive oil and natural gas emissions of nonmethane hydrocarbons include oil spills, refinery processing, and hydraulic fracturing.[11−13]

The mechanisms of photooxidation of VOCs can be affected by the presence of inorganic copollutants, with the effect of NO_x known to be the largest. The effect of SO_2 and NH_3 on the VOC photooxidation is less explored. Several studies have investigated the photooxidation of abundant atmospheric VOCs including isoprene, α-pinene, toluene, 1,3,5-trimethylbenzene, xylene, octane, and gasoline exhaust in the presence of SO_2, and found that it results in the formation of organosulfates ($R-OS(O)_2OH$).[14−20] During photooxidation, SO_2 can be converted to sulfuric acid by hydroxyl radicals (OH),[21] and by

Received: July 1, 2016
Revised: December 6, 2016
Accepted: December 8, 2016
Published: December 8, 2016

DOI: 10.1021/acs.est.6b03304
Environ. Sci. Technol. 2017, 51, 119−127

Table 1. Experimental Conditions for Chamber-Generated Fuel SOA[a]

sample	sample code	precursor	fuel (ppb)	SO_2 (ppb)	NH_3 (ppb)	RH (%)	[SOA] ($\mu g/m^3$)	D_p (nm)
1	DSL/NO_x	DSL	220	0	0	<2	260	169
2	DSL/NO_x/SO_2	DSL	220	200	0	<2	510	178
3	DSL/NO_x/SO_2/NH_3	DSL	220	200	1000	<2	510	176
4	DSL/NO_x/RH	DSL	220	0	0	90	360	162
5	DSL/NO_x/SO_2/RH	DSL	220	200	0	90	470	203
6	BDSL/NO_x	BDSL	160	0	0	<2	45	109
7	BDSL/NO_x/SO_2	BDSL	160	200	0	<2	85	119
8	MIX/NO_x	20% BDSL	32/170	0	0	<2	220	181
9	MIX/NO_x/SO_2	20% BDSL	32/170	200	0	<2	370	162
10	DSL/NO_x[a]	DSL	220	0	0	<2	330	187
11	DSL/NO_x/SO_2[a]	DSL	220	200	0	<2	630	193
12	DSL/NO_x/SO_2-high[a]	DSL	220	570	0	<2	720	195
13	DSL/NO_x/SO_2/NH_3[a]	DSL	220	200	110	<2	530	184

[a]aSample number, sample code name, reactant concentrations, relative humidity (RH), SOA mass concentrations, and particle mean geometric diameters (Dp) are listed. SOA mass concentrations are reported as maxima reached at the end of photooxidation (~3 h). Samples sent through a longer denuder train before collection are labeled with superscript "a".

reactive uptake onto particles involving heterogeneous oxidation of SO_2 by ozone or hydrogen peroxide (H_2O_2).[22] Sulfate seed particles with varying acidity have also been used to generate organosulfates in SOA, where their formation is most prominent under higher acidity.[23−27]

The possible formation routes of organosulfates via reactions of organics with sulfur-containing oxides, acids, and radicals—"sulfate nucleophiles" hereafter—include: (1) epoxide ring opening, (2) addition to protonated carbonyls, (3) substitution of organonitrates, (4) esterification of alcohols, enols, or hydrated hydroperoxides, and (5) radical initiated reactions.[23,28−30] Epoxides can be protonated under acidic conditions making them more susceptible to attack from sulfate nucleophiles, forming β-hydroxysulfates. Similarly, protonated carbonyls can react with sulfate nucleophiles,[29] forming α-hydroxysulfates. Substitution of tertiary organonitrates with sulfate can rapidly occur, even over a full pH range.[31]

Minerath et al.[32] suggested that esterification of alcohols is kinetically hindered at low temperatures of the upper tropospheric aerosols, using methanol as the model alcohol and conducting aqueous experiments. Minerath et al.[32] calculated a rate constant using Kane et al.[33] data and applying similar experimental conditions to be 10 orders of magnitude larger than the self-reported experimental value of Minerath et al.[32] However, this rate constant discrepancy may be due to a difference in experimental design: heterogeneous surface[33] versus homogeneous bulk[32] exposure of methanol to sulfuric acid. Furthermore, it was more recently observed that esterification of alcohols is more efficient in sulfuric acid aerosol than in bulk aqueous solution.[34] In addition to alcohols, carbonyls can be reactive to form organosulfur species. For example, ketones may tautomerize to their enol form and then undergo esterification.[35] Sulfate radicals were proposed by Nozière et al.[36] to form in atmospheric aerosols from the reaction of OH with bisulfate anions. The organosulfate species found in that study were explained by the addition of sulfate radicals to double bonds and further aging by OH.

Although many studies have examined organosulfur formation in the presence of seed aerosols (or bulk solutions) containing sulfuric acid or sulfates, little is known about organosulfur formation pathways through direct reaction of SO_2 with organic species. It has been demonstrated that uptake of SO_2 by oleic acid in the absence of ozone, in the dark, results in direct addition of SO_2 to double bonds.[37] In addition, if ozone is present or formed during photooxidation it can react with alkenes to produce Criegee intermediates which can oxidize SO_2 to SO_3 and indirectly produce organosulfates.[17,38] Under humidified conditions, H_2O_2 could potentially contribute to SO_2 oxidation and SOA formation by heterogeneous chemistry. In summary, although multiple pathways for incorporation of sulfur into SOA organic compounds have been proposed, the relative role of these processes is yet unknown.

In this study, SOA is generated through photooxidation of diesel and biodiesel fuels in chamber experiments to represent photooxidative aging of mixtures similar to liquid diesel composition, such as unburned or evaporated fuel. The effects of relative humidity (RH) and anthropogenic pollutants, NO_x, SO_2, and NH_3, on composition of fuel SOA are investigated. High-resolution nanospray desorption electrospray ionization mass spectrometry (nano-DESI/HRMS) and ultrahigh resolution and mass accuracy capability 21T Fourier transform ion cyclotron resonance mass spectrometry (21T FT-ICR MS), indicate that organosulfur compounds are efficiently produced in the presence of SO_2, without pre-existing sulfate seed aerosols. Unique organosulfur species are categorized into four subsets: compounds with an aliphatic side chain, compounds with formula $C_cH_hSO_3$, compounds with formula $C_cH_hSO_4$, and aromatic compounds. The assigned species are compared to previous field and laboratory studies. Based on our data, some of the organosulfates previously designated as biogenic or of unknown origin in field studies may originate from anthropogenic sources, such as photooxidation of fuel hydrocarbons.

MATERIALS AND METHODS

Fuel Analysis. The composition of diesel fuel (Fluka. No. 2 UST148) and biodiesel fuel (VHG Laboratories, BDBLEND-100P) were analyzed using 2D gas chromatography interfaced with electron impact (EI) and vacuum ultraviolet high-resolution time-of-flight MS (GC-VUV-MS).[39−41] Details of quantification and calibration are given in the Supporting Information (SI), and Figure S1.

Chamber Generation of SOA. Photooxidation of diesel fuel and biodiesel fuel was performed in a 5 m^3 Teflon chamber

DOI: 10.1021/acs.est.6b03304
Environ. Sci. Technol. 2017, 51, 119−127

in the absence of seed particles with added NO and different levels of RH, SO_2, and NH_3 (an example of a time profile of SOA formation is shown in SI Figure S2). Experimental conditions are summarized in Table 1. Photooxidation was driven by radiation from UV−B lamps (FS40T12/UVB, Solarc Systems, Inc.) with an emission centered at 310 nm. A scanning mobility particle sizer (SMPS; TSI 3080 Electrostatic Classifier and TSI 3775 Condensation Particle Counter) and a time-of-flight aerosol mass spectrometer (AMS; Aerodyne) monitored SOA particles formed in the chamber. This study assumed a density of 1.2 g cm^{-3}, which is the median value for densities of SOA reported from anthropogenic precursors.[42] Ozone and NO/NO_y mixing ratios were recorded by a Thermo Scientific model 49*i* ozone analyzer and Thermo Scientific model 42*i*-Y NO_y analyzer, respectively. Further details are provided in the SI.

Filter Collection and Analysis of SOA Samples. The composition of SOA particles was tracked in real time with AMS during most chamber runs. The AMS instrument uses hard EI ionization and causes fragmentation of species, especially organosulfates of interest.[43] Therefore, softer ionization offline techniques with higher mass resolution were also used in this work to unambiguously assign chemical formulas of SOA compounds.

SOA were sent through either a long (3 m) or short (1 m) denuder and collected on poly(tetrafluoroethylene) (PTFE) filters (Millipore, 0.2 μm pore size) via impaction. Filter samples were then sealed and frozen for offline analysis using nano-DESI/HRMS[44] operated in negative mode with a mass-resolving power of $m/\Delta m \approx 1.0 \times 10^5$ at m/z 400. Prior to analysis, frozen filter samples were allowed to equilibrate to room temperature and then unsealed. Acetonitrile (ACN; Fisher, HPLC grade) was used as the working nano-DESI solvent bridge for samples 1−9 and 13 while samples 10−12 were analyzed using a 7:10 (v:v) $ACN:H_2O$ solvent mixture. Several recent field studies of organosulfates used similar solvents for MS analysis.[37,45−47] An additional advantage of nano-DESI compared to the traditional ESI is that it minimizes the solvent/analyte interaction time and therefore minimizes the effect of hydrolysis and other analyte-solvent reactions on the measured SOA composition.[48,49] The spray voltage and heated capillary temperature were 3.5−4 kV and 250−270 °C, respectively. Mass spectra of samples 2, 7, 9, and 10−13 were also recorded using a direct infusion ESI source interfaced with a 21T FT-ICR MS (magnet from Agilent Technologies, Oxford, England; spectrometer built at PNNL) operated in negative mode with a resolving power, sample flow rate, spray voltage, and capillary temperature of $m/\Delta m \approx 1.2 \times 10^6$ at m/z 400, 0.5 μL min^{-1}, 2.4 kV, and 300 °C, respectively. A detailed description of data analysis and processing is reported in the SI.

Several complementary mass spectrometry methods were used in this work. AMS offered real-time mass spectra, making it possible to quantify the overall amount of sulfates in SOA, but not observe individual organosulfate molecules. Nano-DESI/HRMS and 21T FT-ICR MS offered soft ionization, offline filter MS analysis, and provided chemical formulas of individual SOA compounds. The 21T FT-ICR MS had much higher resolving power, mass accuracy, and used longer averaging times compared to the nano-DESI/HRMS instrument, making it possible to detect additional organosulfur species and unambiguously assign higher m/z peaks.

RESULTS AND DISCUSSION

Average Molecular Composition. SI Table S1 summarizes average molecular formulas for the SOA samples based on high-resolution MS analysis. Mass spectral peaks were assigned with $C_cH_hO_oN_nS_s$ elemental formulas with the limits of c = 1−40, h = 2−80, o = 0−35, n = 0−1, and s = 0−1. (Analysis with up to two nitrogen and two sulfur atoms was also performed, but there were very few peaks assigned to n = 2 or s = 2 compounds and the corresponding intensities were <5% the max intensity of the largest peak.) We will refer to families of compounds as CHO, CHON, CHOS, and CHONS depending on the occurrence of the specified atoms in the molecular formula.

The carbon number distribution of aromatics and PAHs in the diesel fuel defined by DBE = 4 and DBE > 4, respectively, from GC analysis is shown in the SI, Figure S3. The distribution is centered around C12, which is larger than the most common size of aromatic compounds observed in SOA (defined in detail in the "Subsets of Organosulfur Species" section below), centered around C8 (SI Figure S3). The higher signal for C8 and C7 aromatic compounds observed in the SOA likely resulted from oxidation pathways for the larger aromatic compounds that led to a loss of aromaticity by ring-opening reactions.

Aside from this specific trend in aromatics, the overall average carbon numbers (SI Table S1) in the DSL SOA were smaller than the average carbon number in the diesel fuel. BDSL SOA also had a smaller average carbon number than the biodiesel fuel, dominated by C_{17} and C_{19} compounds. This observation was consistent with degradation during photo-oxidation of biodiesel fuel.

The high-resolution mass spectra from the DSL/BDSL mixture could be reasonably represented as a linear combination of the individual DSL and BDSL mass spectra (SI Figures S4−S6). However, there was evidence for interference between the DSL and BDSL chemistry from the appearance of new peaks, as well as the distribution of CHOS species (see below).

In general, average O/C and H/C ratios for fuel samples photooxidized in the presence of NO_x did not show any significant difference between DSL, BDSL, and MIX SOA samples (SI Table S2; samples containing SO_2 will be discussed later). The O/C and H/C values from AMS were smaller and larger, respectively, compared to the corresponding nano-DESI/HRMS and 21T FT-ICR MS results. One explanation for this observation is the type of ionization; AMS uses EI whereas nano-DESI/HRMS and 21T FT-ICR MS use soft ionization. Oxygenated species in the AMS can be highly fragmented with ionization and appear to be less oxidized in analysis.[43] Conversely, nano-DESI/HRMS and 21T FT-ICR MS are more selective to oxidized species, making SOA compounds appear to be more oxidized on average. Actual atomic ratios likely fall in between the AMS and HRMS values.

Formation of Organosulfur Species with the Addition of SO_2. There is a clear trend of increasing organosulfur species, CHOS and CHONS, in nano-DESI/HRMS mass spectra with the addition of SO_2 (Figure 1). The intensity weighted percent CHO, CHON, CHOS, and CHONS are presented as pie charts in Figure 1; corresponding values for all SOA samples are listed in SI Table S3. Fractions of CHOS and CHONS peaks increased dramatically with increased SO_2 concentrations. When the amount of SO_2 was almost tripled

DOI: 10.1021/acs.est.6b03304
Environ. Sci. Technol. 2017, 51, 119−127

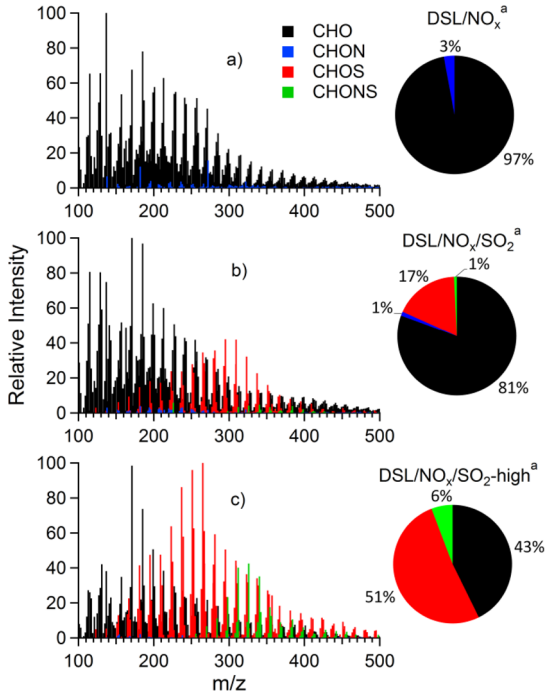

Figure 1. Effect of SO_2 addition on the nano-DESI/HRMS spectra of diesel fuel SOA (longer denuder samples (a) 10, (b) 11, and (c) 12). Peaks are colored by elemental composition. Pie charts are intensity-weighted elemental composition of the peaks.

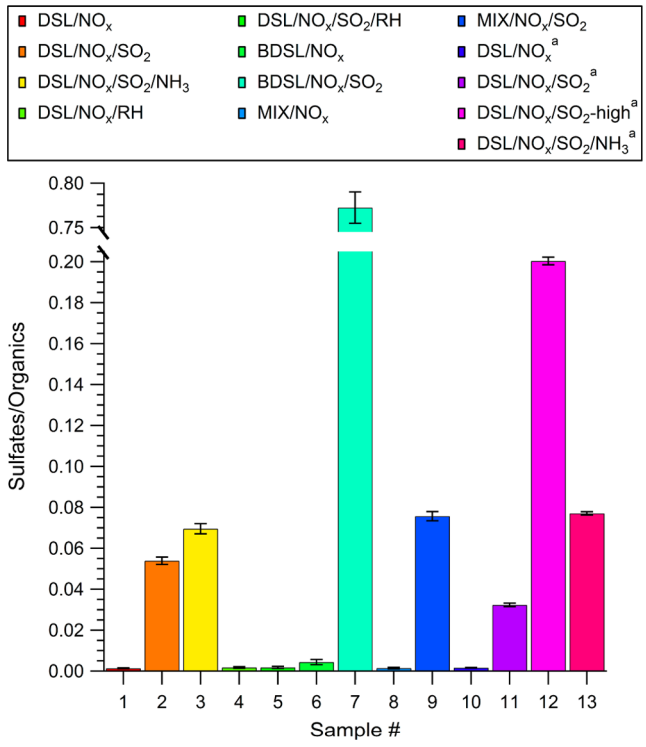

Figure 2. AMS data of SOA samples for particulate sulfates relative to organics. SOA samples are labeled and colored by sample number from Table 1.

from DSL/NO_x/SO_2[a] to DSL/NO_x/SO_2-high[a] the fraction of CHOS also tripled from 17% to 51%, while the fraction of CHONS increased from 1% to 6%. A similar trend with increased amounts of SO_2 was observed for other dry samples (SI Figures S7–S10).

AMS data also supported formation of organosulfur species with addition of SO_2. Experiments in this study were conducted without the presence of sulfate seed to minimize interference between inorganic sulfate and organosulfur species in AMS data. Bar plots of sulfate/organics ratios are reported in Figure 2 (the plot of the nitrates/organics ratios is shown in SI Figure S11). The sulfates/organics ratio increased from samples 2 to 3 and from samples 11 to 13, wherein NH_3 was added to the DSL SOA that already contained SO_2. Although NH_3 could neutralize some of the SOA acidity, it could simultaneously increase the amount of seed aerosol for vapors to condense on. The DSL SOA sample with the largest amount of SO_2 added, sample 12, increased in sulfate/organics ratio relative to sample 11 (as well as sample 2), where less SO_2 was added. The BDSL/NO_x/SO_2 sample (sample 7) had the largest sulfates/organics ratio of all samples; the low BDSL SOA mass concentration (Table 1) was the most likely reason for this effect. The real-time AMS signals for organic and inorganic mass concentrations for the BDSL/NO_x/SO_2, MIX/NO_x/SO_2, and DSL/NO_x/SO_2 samples are shown in SI Figure S12. The major difference between samples is the small organic mass from the BDSL/NO_x/SO_2 sample. As the amount of BDSL/NO_x SOA was smaller than the other samples, any additional SOA formed from the presence of SO_2 would have had a larger effect on the sulfates/organics ratio. Although the MIX/NO_x/SO_2 sample only contained 20% biodiesel, it was enough to increase the sulfates/organics ratio from the DSL/NO_x/SO_2 sample.

SO_2 addition made compounds with lower double bond equivalent (DBE, the combined number of double bonds and rings in the molecule; eq 1) appear more prominently in the ESI mass spectra. SI Figure S13, which plots DBE as a function of carbon number, along with trends of common species (described in SI Table S4) shows that with the increase in SO_2 the relative contribution of low DBE values clearly increases. In fact, DBE = 0 compounds, with no C═C and C═O double bonds or rings, become visible in samples containing SO_2 (note that sulfate−$OS(O)_2OH$ and sulfonate−$S(O)_2OH$ groups do not contribute to DBE calculated with eq 1 (because the calculation assumes valence of 2 for sulfur). Average DBE values listed in SI Table S1 also decrease with the SO_2 addition. Most likely, this is the effect of converting poorly ionizable molecules with low oxidation states into organosulfur compounds that ionize more readily.

$$\mathrm{DBE} = 1 + C - \frac{H}{2} + \frac{N}{2} \quad (1)$$

Formation of organosulfates by sulfuric acid mediated mechanisms requires water. Although most SOA samples were prepared under dry conditions (RH < 2%), residual water from the chamber and also that from addition of the aqueous H_2O_2 solution may have been sufficient to form sulfuric acid and sulfate nucleophiles. There is also a possibility that organic particles dissolved some of the SO_2 and SO_3 formed in the chamber to further promote heterogeneous sulfuric acid and organosulfur species formation. As previously mentioned, SO_2 can react directly with organics by addition to double bonds.[17,37,38] SO_2 may also be oxidized to SO_3 by Criegee intermediates which may be present in the chamber once ozone is produced. Addition of SO_2 promotes formation of organo-

DOI: 10.1021/acs.est.6b03304
Environ. Sci. Technol. 2017, 51, 119−127

sulfates by increasing the acidity of the particles, but also, in turn, by increasing the amount of available nucleophiles.

Comparison of the dry DSL/NO_x and DSL/NO_x/SO_2 samples indicates that addition of SO_2 resulted in an increase in C, H, O/C, and H/C and a decrease in DBE (SI Tables S1 and S2). Increase in the degree of oxidation is most likely attributed to addition of either a sulfate or sulfonate group, which carry several oxygen atoms. The dry BDSL/NO_x and BDSL/NO_x/SO_2 samples show a similar trend. In contrast, average oxidation level for the DSL/NO_x/SO_2/RH sample (prepared under humid conditions) decreased. Furthermore, the amount of sulfur observed in this sample was lower than in other samples with added SO_2. Notably, the DSL/NO_x/SO_2/RH sample did not contain abundant CHOS or CHONS species, unlike the other samples. There are two possible explanations for this interesting effect of high humidity in SOA composition. One likely explanation is that high humidity, while promoting the conversion of SO_2 into sulfuric acid in the chamber, actually reduced the effective acidity in the particles by diluting them with water. The decrease in acidity must be sufficient to prevent acid-catalyzed reactions that occurred in the drier samples. For example, the presence of water in high humidity experiments may suppress sulfate esterification reactions of hydroxyl groups. The partial wall loss of SO_2 and H_2SO_4 is another possible reason for this observation in high humidity experiments. The wall loss of highly water-soluble compounds increases at high RH because they can partition into the water film on the chamber walls.[50] The reduction in the concentration of sulfuric acid could then reduce the yield of organosulfates. This effect did not seem to affect the overall amount of organic compounds as the observed SOA mass concentrations under the dry and humid conditions were comparable (Table 1). Clearly, the effect of humidity on DSL and BDSL oxidation is complicated and deserves further study.

Subsets of Organosulfur Species. A list of all CHOS mass spectral peaks observed in the samples is provided in the Supporting Information. The CHOS species were separated into four subsets. "*Subset A*" includes aliphatic species based on the definition of "aliphatic" introduced in the recent study by Tao et al.[51] Specifically, CHOS species with C > 8, DBE < 3, and 3 < O < 7 belong to this class. "*Subset B*" includes species with the formula $C_cH_hSO_3$, which do not contain enough oxygen atoms to be organosulfates. "*Subset C*" has the formula $C_cH_hSO_4$, which could be interpreted as one sulfate group attached to an oxygen-free substituent or a sulfonate group attached to a substituent containing a single oxygen atom. "*Subset D*" includes aromatic species identified by a high aromaticity index (AI).[52,53] The concept of AI was developed for a broad range of organic molecules, and showed that compounds with AI ≥ 0.5 are likely to be aromatic. As pointed out in the original paper, it does not work well for molecules containing a large number of oxygen atoms.[51] Organosulfates, which can be viewed as a result of a replacement of (C)OH with (C)OSO_3H, and sulfonates, resulting from a replacement of (C)H by (C)SO_3H, contain a sulfur atom and three O atoms that do not affect the aromaticity of the rest of the molecule. Counting these atoms in the originally proposed AI formula would result in incorrect conclusions about the aromaticity of the molecule, for example, the calculated value for benzenesulfonic acid, $C_6H_6SO_3$, would be AI = 0 instead of the AI* = 0.67 expected for a substituted benzene ring. To account for this effect in CHOS species, we redefined AI in this paper by excluding the SO_3 set of atoms from the AI calculations. The modified equation is (where O* = O 3):

$$AI^* = \frac{DBE - O^*}{C - O^*} \quad (2)$$

The distribution of *subsets A, B, C,*, and *D* between samples is listed in SI Table S5. Note that some molecules fit the description of more than one subset, so percentages in SI Table S4 do not add up to 100%. For example, an aromatic organosulfate would be described as fitting both *subset B* and *D*. DSL SOA samples DSL/NO_x/SO_2, DSL/NO_x/SO_2/NH_3, DSL/NO_x/SO_2[a], DSL/NO_x/SO_2-high[a], and DSL/NO_x/SO_2/NH_3[a] contained a large number of aliphatic CHOS species (*subset A*). Van Krevelen plots of DSL/NO_x/SO_2[a] and DSL/NO_x/SO_2-high[a] for CHOS species are shown in SI Figure S14; *subset A* compounds are highlighted in red. These compounds were also observed in the CH_2–Kendrick diagram shown in Figure 3, which features prominent families of compounds with

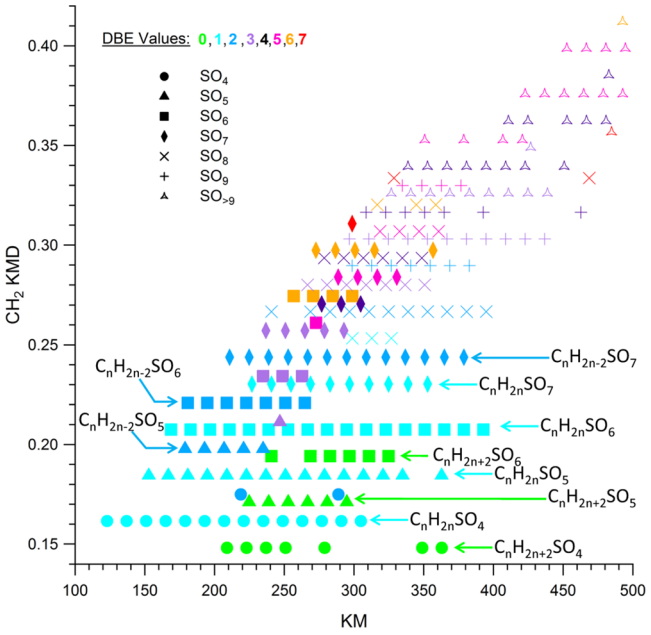

Figure 3. CH_2–Kendrick mass defect plot for CHOS species of DSL/NO_x/SO_2[a], sample 11. The mass spectral peaks are colored by DBE and shaped by the total number, *x*, of oxygen atoms (as SO_x). Prominent families are labeled with general chemical formulas.

low DBE. These compounds had high mass spectral overlap with the compounds found in Shanghai particulate matter by Tao et al.,[51] who proposed an esterification mechanism for their formation as well as possible contribution from primary sources. Dry DSL SOA samples produced in the presence of NH_3 contained the largest percentage of aliphatic CHOS species (about 60% of detected CHOS were in *subset A*), whereas the fraction of these species in humid DSL SOA and dry BDSL SOA samples was the lowest (<2%). The effect of humidity can be attributed to the suppression of esterification by particle water, as discussed above. The effect of NH_3 is counterintuitive as it is expected to reduce the particle acidity by neutralizing sulfuric acid and suppress the esterification processes. On the other hand, presence of NH_3 increases the overall amount of sulfate nucleophiles in the particles by forming ammonium sulfate. It seems that the second effect is more important because average sulfur content increases with

DOI: 10.1021/acs.est.6b03304
Environ. Sci. Technol. 2017, 51, 119–127

addition of NH_3 (SI Table S1). The reason for low abundance of *subset A* compounds in the BDSL sample is unclear.

Subset B compounds, which contain one sulfur atom and three oxygen atoms, most likely correspond to organosulfonates ($R-SO_3H$) which were recently observed in chamber experiments.[24] The MIX/NO_x/SO_2 and DSL/NO_x/SO_2/RH had the largest fraction of CHOS *subset B* compounds, whereas the other samples had less than 2%. The high humidity DSL/NO_x/SO_2/RH sample had a large peak (35% RI) corresponding to benzenesulfonic acid. The most abundant sulfonates in MIX/NO_x/SO_2 sample were $C_{21}H_{14}SO_3$ (18% RI), $C_{23}H_{18}SO_3$ (90% RI), $C_{24}H_{20}SO_3$ (100% RI, i.e., the largest peak in the spectrum), $C_{25}H_{22}SO_3$ (71% RI), and $C_{26}H_{14}SO_3$ (38% RI). All of these species have the same general formula $C_nH_{2n-28}SO_3$, with DBE values of 15. These compounds likely correspond to sulfonates of substituted benzopyrene ($C_{20}H_{12}$, DBE = 15).

The $C_cH_hSO_4$ species in *subset C*, which may be either hydroxy or keto-sulfonates or organosulfates, were most abundant in the DSL/NO_x/SO_2/RH sample. Considering that the same sample also contained a high fraction of *subset B* compounds, assigned to sulfonates, it is reasonable to assume that keto- and hydroxyl- sulfonates contribute to *subset C*. The DSL SOA sample with the largest amount of added SO_2, sample 12, had the largest intensity peaks for *subset C* and showed a clear pattern of the molecular formulas of $C_nH_{2n}SO_4$ for $2 < n < 15$, which could be keto-sulfonates of saturated compounds or sulfates of unsaturated ones. Less intense mass spectral peaks of these molecular formulas were also seen in sample 11, DSL/NO_x/SO_2[a], (Figure 3) as well as other DSL SOA samples, except for the high humidity DSL/NO_x/SO_2/RH sample.

The sample with the highest fraction of aromatic CHOS (*subset D*) was MIX/NO_x/SO_2; all other samples had fewer than 5% of CHOS species from this group. We mentioned above that aromatics in diesel fuel appeared to undergo ring-opening reactions that shifted the average carbon number to lower values and reduced the degree of aromaticity. The addition of biodiesel fuel to diesel fuel had an inhibitory effect on these reactions, resulting in a larger fraction of aromatic products. Interestingly, the largest aromatic species of MIX/NO_x/SO_2 were also organosulfonates, the same peaks previously emphasized for *subset C*. It is likely that aromatic sulfonates undergo ring-opening reactions after being further oxidized and that the presence of reactive biodiesel components competes with this secondary oxidation of aromatic CHOS. Reaction rates and product stability may also favor smaller aromatic CHOS. It should be pointed out that *subset B* and *D* in MIX/NO_x/SO_2 appeared to be much less abundant in 21T FT-ICR MS data for reasons that are presently unclear.

Comparison of CHOS Species with Previous Literature. There is a substantial overlap of organosulfur mass spectral peaks observed in this fuel photooxidation study with previous reports from both field and chamber measurements.[23,24,46,51,54−58] Figure 4 shows a DBE versus carbon number plot comparing the CHOS species observed in a few selected studies with the *same* species in DSL/NO_x/SO_2 (sample 2). Most of the aliphatic CHOS species detected in the urban environment of Shanghai and Los Angeles by Tao et al.[51] were also observed in the DSL SOA samples in this study. For example, we observed the $C_nH_{2n+2}SO_4$ family of compounds (Figure 3, light blue solid circles) that represented a dominant family of organosulfur species in Tao et al.[51] Note

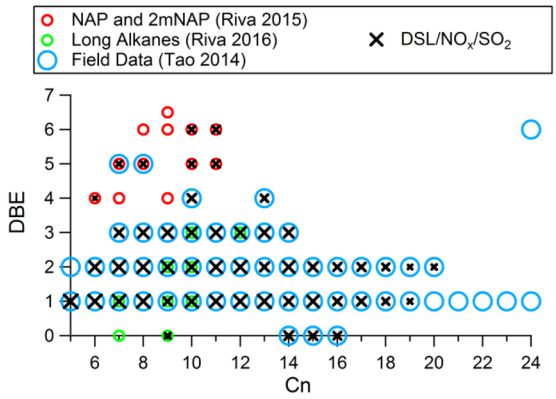

Figure 4. Carbon number distribution for CHOS species observed by Tao et al. (2014)[51] and Riva et al. (2015)[24] and (2016)[23] where points are colored by source. Data from this study for the diesel SOA sample 2 (× 's) are only included in the plot when the formula overlaps with one of the formulas previously reported in the literature. The size of the "×" marker is logarithmically weighed by the observed peak intensity.

that we are not suggesting that *only* DSL SOA is responsible for mass spectra in Tao et al.,[51] but that data in this study have high overlap, especially with aliphatic organosulfur species. There was also overlap of organosulfur species between this study and the field study by Peng et al.[54] for chemical formulas $C_nH_{2n}SO_5$ and $C_nH_{2n-2}SO_5$ (Figure 3, light blue solid triangles and dark blue solid triangles, respectively), especially in the Guongzhou urban Pearl River Delta samples. Previous data on laboratory-generated SOA of long alkanes,[23] and SOA of naphthalene (NAP) and 2-methyl-naphthalene (2 mNAP)[24] by Riva and coauthors are also included in this comparison. The largest overlap of DSL/NO_x/SO_2 with aromatic compounds reported by Riva et al.[24] was observed for organosulfate peaks of the type $C_nH_{2n-10}SO_{6-7}$ with DBE values of 6 from both NAP ($C_{10}H_{10}SO_7$ and $C_{10}H_{10}SO_6$) and 2 mNAP ($C_{11}H_{12}SO_7$) SOA.

As mentioned earlier, fewer organosulfur species are observed in mass spectra for high humidity samples. This may be due to a dilution of sulfate nucleophiles by aerosol liquid water, as well as a decrease in the acidity.[57] Interestingly, $C_7H_6SO_5$ and $C_8H_8SO_5$ are the most abundant peaks in the high humidity sample, DSL/NO_x/SO_2/RH, that overlapped with species reported by both Tao et al.[51] data and Riva et al.[24] These peaks had DBE values of 5 and were of the general chemical formula $C_nH_{2n-8}SO_5$, which Riva et al.[24] attributed to organosulfonates in the 2 mNAP SOA. Riva et al.[24] reported that, in general, RH appeared to have little effect on the formation of sulfonates and organosulfates for 2 mNAP SOA. However, in the specific case of $C_7H_6SO_5$ and $C_8H_8SO_5$ found in our high humidity samples, their concentrations increased with increasing the RH for each specific acidity (Riva et al.[24] samples from 10/20/2014 and 10/25/2014). The aromatic peak observed in the high humidity sample that was also reported by Riva et al.,[24] $C_6H_6SO_4$, most likely corresponds to hydroxybenzene sulfonic acid. The largest overlap of the BDSL SOA sample was with Tao et al.[51] data for peaks of $C_6H_{10}SO_6$ (also the most intense CHOS peak in general), $C_6H_{12}SO_6$, and $C_8H_{16}SO_6$.

Atmospheric Implications. This is the first study of organosulfates in SOA formed in the photooxidation of diesel and biodiesel fuels. We observed that the presence of SO_2 increased the size of SOA particles and formed numerous

DOI: 10.1021/acs.est.6b03304
Environ. Sci. Technol. 2017, 51, 119−127

organosulfur species, even under dry conditions. Suppression of organosulfur compounds under humidified conditions was not expected because most previous studies have observed higher yields of organosulfur species at elevated RH. However, a majority of these studies employed sulfate-containing seed particles that may obscure several important organosulfur formation pathways that are unique to SO_2 chemistry, such as direct addition of SO_2 to unsaturated species.[37] It is possible that this result may be influenced by the increased wall loss of sulfuric acid at elevated RH; ideally these experiments should be repeated with instruments capable of explicit sulfuric acid concentration measurements. The substantial overlap of organosulfur species observed in this study with previous field studies suggests that these alternative mechanisms of organosulfur formation could be important in the atmosphere, and they require additional scrutiny. We should point out that ionization of organosulfates is especially favorable in the negative-ion mode ESI and DESI, and this may make the fraction of organosulfates appear larger than it actually is in the particles. The observed fraction of organosulfates is further amplified by the high SO_2 concentrations used in this study. The organosulfates formed in ambient particles by the same VOC + SO_2 + NO_x photooxidation mechanisms may therefore be minority species. Future photooxidation experiments with single components of fuel precursors combined with tandem MS analysis are necessary to determine the actual yields of these organosulfur species.

Many organosulfur species in field data previously classified as biogenic or species of unknown origin were also found among the products of photooxidation of diesel and biodiesel fuel in this study. For example, the organosulfur peak $C_5H_{10}SO_5$ was previously assigned to either unknown[55] or isoprene[51] origin and another peak, $C_9H_{16}SO_7$, was assigned as a product of limonene[55,56] or other monoterpene precursors.[51] Both of these formulas were prominently present in the DSL SOA mass spectra suggesting that they could also be of anthropogenic origin. The SI Excel file provides a number of other examples of the overlap of CHOS species with those observed in previous measurements. These results show that the origin of organosulfur species cannot be based only on their formula.

■ ASSOCIATED CONTENT

Supporting Information

The Supporting Information is available free of charge on the ACS Publications website at DOI: 10.1021/acs.est.6b03304.

Further information on the analysis of fuel samples, chamber experiments, and the processing of high-resolution mass spectra. Also includes multiple figures and tables describing photooxidation of a mixture of diesel and biodiesel fuels, high-resolution mass spectra for different types of SOA samples, comparison of C-number distribution of aromatic compounds in fuel and fuel SOA, AMS measurements of organic and inorganic species during SOA formation, AMS nitrate/organics ratios, distribution of DBE values for the observed SOA compounds, Van Krevelen diagrams for the CHOS species, elemental composition of SOA, and distribution of the observed organosulfur species into classes discussed in this paper (PDF)

An Excel table of all the organosulfur species observed in the samples (XLSX)

■ AUTHOR INFORMATION

Corresponding Author

*Phone: (949) 824-1262; fax: (949) 824-2420; e-mail: nizkorod@uci.edu.

ORCID

Greg T. Drozd: 0000-0002-9195-6360

Sergey A. Nizkorodov: 0000-0003-0891-0052

Notes

The authors declare no competing financial interest.

■ ACKNOWLEDGMENTS

S.B. acknowledges support from the NSF grant AGS-1227579. P.L., A.L., J.L., A.M., and S.N. acknowledge support by the U.S. Department of Commerce, National Oceanic and Atmospheric Administration through Climate Program Office's AC4 program, award NA13OAR4310066/NA13OAR4310062. The AMS instrument was acquired with the NSF grant MRI-0923323. GD and AG acknowledge use of the Chemical Dynamics Beamline 9.0.2. at the Advanced Light Source at LBNL supported by the Director, Office of Science, Office of Basic Energy Sciences, of the U.S. Department of Energy under Contract No. DE-AC02-05CH11231. Mass spectrometry measurements were performed at the W.R. Wiley Environmental Molecular Sciences Laboratory (EMSL), a national scientific user facility located at PNNL, and sponsored by the Office of Biological and Environmental Research of the U.S. DOE. PNNL is operated for US DOE by Battelle Memorial Institute under Contract No. DEAC06-76RL0 1830.

■ REFERENCES

(1) Wang, K.; Dickinson, R. E.; Liang, S. Clear sky visibility has decreased over land globally from 1973 to 2007. *Science* **2009**, *323* (5920), 1468−1470.

(2) Pope, I. C.; Burnett, R. T.; Thun, M. J.; Calle, E. E.; Krewski, D.; Ito, K.; Thurston, G. D. Lung cancer, cardiopulmonary mortality, and long-term exposure to fine particulate air pollution. *JAMA* **2002**, *287* (9), 1132−1141.

(3) IPCC. Summary for policymakers. In *Climate Change 2013: The Physical Science Basis. Contribution of Working Group I to the Fifth Assessment Report of the Intergovernmental Panel on Climate Change*; Stocker, T. F., Qin, D., Plattner, G.-K., Tignor, M., Allen, S. K., Boschung, J., Nauels, A., Xia, Y., Bex, V., Midgley, P. M., Eds.; Cambridge University Press: Cambridge, 2013.

(4) Goldstein, A. H.; Galbally, I. E. Known and unexplored organic constituents in the Earth's atmosphere. *Environ. Sci. Technol.* **2007**, *41* (5), 1514−1521.

(5) Zhang, Q.; Jimenez, J. L.; Canagaratna, M. R.; Allan, J. D.; Coe, H.; Ulbrich, I.; Alfarra, M. R.; Takami, A.; Middlebrook, A. M.; Sun, Y. L.; Dzepina, K.; Dunlea, E.; Docherty, K.; DeCarlo, P. F.; Salcedo, D.; Onasch, T.; Jayne, J. T.; Miyoshi, T.; Shimono, A.; Hatakeyama, S.; Takegawa, N.; Kondo, Y.; Schneider, J.; Drewnick, F.; Borrmann, S.; Weimer, S.; Demerjian, K.; Williams, P.; Bower, K.; Bahreini, R.; Cottrell, L.; Griffin, R. J.; Rautiainen, J.; Sun, J. Y.; Zhang, Y. M.; Worsnop, D. R. C. L. Ubiquity and dominance of oxygenated species in organic aerosols in anthropogenically-influenced Northern Hemisphere midlatitudes. *Geophys. Res. Lett.* **2007**, *34*, L13801 DOI: 10.1029/2007GL029979.

(6) Glasius, M.; Goldstein, A. H. Recent discoveries and future challenges in atmospheric organic chemistry. *Environ. Sci. Technol.* **2016**, *50* (6), 2754−2764.

(7) Zhang, R.; Wang, G.; Guo, S.; Zamora, M. L.; Ying, Q.; Lin, Y.; Wang, W.; Hu, M.; Wang, Y. Formation of urban fine particulate matter. *Chem. Rev.* **2015**, *115* (10), 3803−3855.

(8) Gentner, D. R.; Isaacman, G.; Worton, D. R.; Chan, A. W. H.; Dallmann, T. R.; Davis, L.; Liu, S.; Day, D. A.; Russell, L. M.; Wilson,

K. R.; Weber, R.; Guha, A.; Harley, R. A.; Goldstein, A. H. Elucidating secondary organic aerosol from diesel and gasoline vehicles through detailed characterization of organic carbon emissions. *Proc. Natl. Acad. Sci. U. S. A.* **2012**, *109* (45), 18318−18323.
(9) Fukagawa, N. K.; Li, M.; Poynter, M. E.; Palmer, B. C.; Parker, E.; Kasumba, J.; Holmen, B. A. Soy biodiesel and petrodiesel emissions differ in size, chemical composition and stimulation of inflammatory responses in cells and animals. *Environ. Sci. Technol.* **2013**, *47* (21), 12496−12504.
(10) Gordon, T. D.; Presto, A. A.; May, A. A.; Nguyen, N. T.; Lipsky, E. M.; Donahue, N. M.; Gutierrez, A.; Zhang, M.; Maddox, C.; Rieger, P.; Chattopadhyay, S.; Maldonado, H.; Maricq, M. M.; Robinson, A. L. Secondary organic aerosol formation exceeds primary particulate matter emissions for light-duty gasoline vehicles. *Atmos. Chem. Phys.* **2014**, *14* (9), 4661−4678.
(11) Drozd, G. T.; Worton, D. R.; Aeppli, C.; Reddy, C. M.; Zhang, H.; Variano, E.; Goldstein, A. H. Modeling comprehensive chemical composition of weathered oil following a marine spill to predict ozone and potential secondary aerosol formation and constrain transport pathways. *J. Geophys. Res.: Oceans* **2015**, *120* (11), 7300−7315.
(12) Field, R. A.; Soltis, J.; McCarthy, M. C.; Murphy, S.; Montague, D. C. Influence of oil and gas field operations on spatial and temporal distributions of atmospheric non-methane hydrocarbons and their effect on ozone formation in winter. *Atmos. Chem. Phys.* **2015**, *15* (6), 3527−3542.
(13) Altieri, K. E.; Stone, A. Prospective air pollutant emissions inventory for the development and production of unconventional natural gas in the Karoo basin, South Africa. *Atmos. Environ.* **2016**, *129*, 34−42.
(14) Edney, E. O.; Kleindienst, T. E.; Jaoui, M.; Lewandowski, M.; Offenberg, J. H.; Wang, W.; Claeys, M. Formation of 2-methyl tetrols and 2-methylglyceric acid in secondary organic aerosol from laboratory irradiated isoprene/NO_X/SO_2/air mixtures and their detection in ambient $PM_{2.5}$ samples collected in the eastern United States. *Atmos. Environ.* **2005**, *39* (29), 5281−5289.
(15) Jaoui, M.; Edney, E. O.; Kleindienst, T. E.; Lewandowski, M.; Offenberg, J. H.; Surratt, J. D.; Seinfeld, J. H. Formation of secondary organic aerosol from irradiated α-pinene/toluene/NO_x mixtures and the effect of isoprene and sulfur dioxide. *J. Geophys. Res.* **2008**, *113*, D09303 DOI: 10.1029/2007JD009426.
(16) Praplan, A. P.; Hegyi-Gaeggeler, K.; Barmet, P.; Pfaffenberger, L.; Dommen, J.; Baltensperger, U. Online measurements of water-soluble organic acids in the gas and aerosol phase from the photooxidation of 1,3,5-trimethylbenzene. *Atmos. Chem. Phys.* **2014**, *14* (16), 8665−8677.
(17) Liu, T.; Wang, X.; Hu, Q.; Deng, W.; Zhang, Y.; Ding, X.; Fu, X.; Bernard, F.; Zhang, Z.; Lu, S.; He, Q.; Bi, X.; Chen, J.; Sun, Y.; Yu, J.; Peng, P.; Sheng, G.; Fu, J. Formation of secondary aerosols from gasoline vehicle exhaust when mixing with SO_2. *Atmos. Chem. Phys.* **2016**, *16* (2), 675−689.
(18) Santiago, M.; Vivanco, M. G.; Stein, A. F. SO_2 effect on secondary organic aerosol from a mixture of anthropogenic VOCs: Experimental and modeled results. *Int. J. Environ. Pollut.* **2012**, *50* (1/2/3/4), 224−233.
(19) Kleindienst, T. E.; Edney, E. O.; Lewandowski, M.; Offenberg, J. H.; Jaoui, M. Secondary organic carbon and aerosol yields from the irradiations of isoprene and α-pinene in the presence of NO_x and SO_2. *Environ. Sci. Technol.* **2006**, *40* (12), 3807−3812.
(20) Friedman, B.; Brophy, P.; Brune, W. H.; Farmer, D. K. Heterogeneous reactions of glyoxal on particulate matter: Identification of acetals and sulfate esters. *Environ. Sci. Technol.* **2005**, *39* (6), 1532−1541.
(21) Finlayson-Pitts, B. J.; Pitts, J. N. *Chemistry of the Upper and Lower Atmosphere: Theory, Experiments, And Applications*; Academic Press: San Diego, CA, 2000.
(22) Li, L.; Chen, Z. M.; Zhang, Y. H.; Zhu, T.; Li, J. L.; Ding, J. Kinetics and mechanism of heterogeneous oxidation of sulfur dioxide by ozone on surface of calcium carbonate. *Atmos. Chem. Phys.* **2006**, *6* (9), 2453−2464.
(23) Riva, M.; Da Silva Barbosa, T.; Lin, Y. H.; Stone, E. A.; Gold, A.; Surratt, J. D. Characterization of organosulfates in secondary organic aerosol derived from the photooxidation of long-chain alkanes. *Atmos. Chem. Phys.* **2016**, *16* (17), 11001−11018.
(24) Riva, M.; Tomaz, S.; Cui, T.; Lin, Y.-H.; Perraudin, E.; Gold, A.; Stone, E. A.; Villenave, E.; Surratt, J. D. Evidence for an unrecognized secondary anthropogenic source of organosulfates and sulfonates: Gas-phase oxidation of polycyclic aromatic hydrocarbons in the presence of sulfate aerosol. *Environ. Sci. Technol.* **2015**, *49* (11), 6654−6664.
(25) Surratt, J. D.; Lewandowski, M.; Offenberg, J. H.; Jaoui, M.; Kleindienst, T. E.; Edney, E. O.; Seinfeld, J. H. Effect of acidity on secondary organic aerosol formation from isoprene. *Environ. Sci. Technol.* **2007**, *41* (15), 5363−5369.
(26) Chan, M. N.; Surratt, J. D.; Chan, A. W. H.; Schilling, K.; Offenberg, J. H.; Lewandowski, M.; Edney, E. O.; Kleindienst, T. E.; Jaoui, M.; Edgerton, E. S.; Tanner, R. L.; Shaw, S. L.; Zheng, M.; Knipping, E. M.; Seinfeld, J. H. Influence of aerosol acidity on the chemical composition of secondary organic aerosol from β-caryophyllene. *Atmos. Chem. Phys.* **2011**, *11* (4), 1735−1751.
(27) Drozd, G. T.; Woo, J. L.; McNeil, V. F. Self-limited uptake of α-pinene-oxide to acidic aerosol: the effects of liquid-liquid phase separation and implications for the formation of secondary organic aerosol and organosulfates from epoxides. *Atmos. Chem. Phys.* **2013**, *13* (16), 8255−8263.
(28) Kundu, S.; Quraishi, T. A.; Yu, G.; Suarez, C.; Keutsch, F. N.; Stone, E. A. Evidence and quantitation of aromatic organosulfates in ambient aerosols in Lahore, Pakistan. *Atmos. Chem. Phys.* **2013**, *13* (9), 4865−4875.
(29) McNeill, V. F.; Woo, J. L.; Kim, D. D.; Schwier, A. N.; Wannell, N. J.; Sumner, A. J.; Barakat, J. M. Aqueous-phase secondary organic aerosol and organosulfate formation in atmospheric aerosols: A modeling study. *Environ. Sci. Technol.* **2012**, *46* (15), 8075−8081.
(30) Berndt, T.; Stratmann, F.; Braesel, S.; Heintzenberg, J.; Laaksonen, A.; Kulmala, M. SO_2 oxidation products other than H_2SO_4 as a trigger of new particle formation. Part 1: Laboratory investigations. *Atmos. Chem. Phys.* **2008**, *8* (21), 6365−6374.
(31) Darer, A. I.; Cole-Filipiak, N. C.; O'Connor, A. E.; Elrod, M. J. Formation and stability of atmospherically relevant isoprene-derived organosulfates and organonitrates. *Environ. Sci. Technol.* **2011**, *45* (5), 1895−1902.
(32) Minerath, E. C.; Casale, M. T.; Elrod, M. J. Kinetics feasibility study of alcohol sulfate esterification reactions in tropospheric aerosols. *Environ. Sci. Technol.* **2008**, *42* (12), 4410−4415.
(33) Kane, S. M.; Leu, M.-T. Uptake of methanol vapor in sulfuric acid solutions. *J. Phys. Chem. A* **2001**, *105* (9), 1411−1415.
(34) Li, J.; Jang, M. Kinetic study of esterification of sulfuric acid with alcohols in aerosol bulk phase. *Atmos. Chem. Phys. Discuss.* **2013**, *13* (9), 23217−23250.
(35) Nguyen, T. B.; Lee, P. B.; Updyke, K. M.; Bones, D. L.; Laskin, J.; Laskin, A.; Nizkorodov, S. A. Formation of nitrogen- and sulfur-containing light-absorbing compounds accelerated by evaporation of water from secondary organic aerosols. *J. Geophys. Res.: Atmospheres* **2012**, *117*, D01207 DOI: 10.1029/2011JD016944.
(36) Nozière, B.; Ekström, S.; Alsberg, T.; Holmström, S. C. L. Radical-initiated formation of organosulfates and surfactants in atmospheric aerosols. *Geophys. Res. Lett.* **2010**, *37*, L05806 DOI: 10.1029/2009GL041683.
(37) Shang, J.; Passananti, M.; Dupart, Y.; Ciuraru, R.; Tinel, L.; Rossignol, S. P.; Perrier, S. B.; Zhu, T.; George, C. SO_2 Uptake on oleic acid: A new formation pathway of organosulfur compounds in the atmosphere. *Environ. Sci. Technol. Lett.* **2016**, *3* (2), 67−72.
(38) Mauldin, R. L., III; Berndt, T.; Sipila, M.; Paasonen, P.; Petaja, T.; Kim, S.; Kurten, T.; Stratmann, F.; Kerminen, V. M.; Kulmala, M. A new atmospherically relevant oxidant of sulphur dioxide. *Nature* **2012**, *488* (7410), 193−196.
(39) Isaacman, G.; Wilson, K. R.; Chan, A. W. H.; Worton, D. R.; Kimmel, J. R.; Nah, T.; Hohaus, T.; Gonin, M.; Kroll, J. H.; Worsnop, D. R.; Goldstein, A. H. Improved resolution of hydrocarbon structures and constitutional isomers in complex mixtures using gas chromatog-

raphy-vacuum ultraviolet-mass spectrometry. *Anal. Chem.* **2012**, *84* (5), 2335−2342.
(40) Worton, D. R.; Isaacman, G.; Gentner, D. R.; Dallmann, T. R.; Chan, A. W. H.; Ruehl, C.; Kirchstetter, T. W.; Wilson, K. R.; Harley, R. A.; Goldstein, A. H. Lubricating oil dominates primary organic aerosol emissions from motor vehicles. *Environ. Sci. Technol.* **2014**, *48* (7), 3698−3706.
(41) Worton, D. R.; Zhang, H.; Isaacman-VanWertz, G.; Chan, A. W. H.; Wilson, K. R.; Goldstein, A. H. Comprehensive chemical characterization of hydrocarbons in NIST standard reference material 2779 Gulf of Mexico crude oil. *Environ. Sci. Technol.* **2015**, *49* (22), 13130−13138.
(42) Hallquist, M.; Wenger, J. C.; Baltensperger, U.; Rudich, Y.; Simpson, D.; Claeys, M.; Dommen, J.; Donahue, N. M.; George, C.; Goldstein, A. H.; Hamilton, J. F.; Herrmann, H.; Hoffmann, T.; Iinuma, Y.; Jang, M.; Jenkin, M. E.; Jimenez, J. L.; Kiendler-Scharr, A.; Maenhaut, W.; McFiggans, G.; Mentel, T. F.; Monod, A.; Prévôt, A. S. H.; Seinfeld, J. H.; Surratt, J. D.; Szmigielski, R.; Wildt, J. The formation, properties and impact of secondary organic aerosol: current and emerging issues. *Atmos. Chem. Phys.* **2009**, *9* (14), 5155−5236.
(43) Farmer, D. K.; Matsunaga, A.; Docherty, K. S.; Surratt, J. D.; Seinfeld, J. H.; Ziemann, P. J.; Jimenez, J. L. Response of an aerosol mass spectrometer to organonitrates and organosulfates and implications for atmospheric chemistry. *Proc. Natl. Acad. Sci. U. S. A.* **2010**, *107* (15), 6670−6675.
(44) Laskin, J.; Eckert, P. A.; Roach, P. J.; Heath, B. S.; Nizkorodov, S. A.; Laskin, A. Chemical analysis of complex organic mixtures using reactive nanospray desorption electrospray ionization mass spectrometry. *Anal. Chem.* **2012**, *84* (16), 7179−7187.
(45) Shalamzari, M. S.; Vermeylen, R.; Blockhuys, F.; Kleindienst, T. E.; Lewandowski, M.; Szmigielski, R.; Rudzinski, K. J.; Spólnik, G.; Danikiewicz, W.; Maenhaut, W.; Claeys, M. Characterization of polar organosulfates in secondary organic aerosol from the unsaturated aldehydes 2-E-pentenal, 2-E-hexenal, and 3-Z-hexenal. *Atmos. Chem. Phys.* **2016**, *16* (11), 7135−7148.
(46) Kuang, B. Y.; Lin, P.; Hu, M.; Yu, J. Z. Aerosol size distribution characteristics of organosulfates in the Pearl River Delta region, China. *Atmos. Environ.* **2016**, *130*, 23−35.
(47) Hettiyadura, A. P. S.; Jayarathne, T.; Baumann, K.; Stone, E. A. Qualitative and quantitative analysis of atmospheric organosulfates in Centreville, Alabama. *Atmos. Chem. Phys. Discuss.* **2016**, 1−26.
(48) Laskin, J.; Laskin, A.; Roach, P. J.; Slysz, G. W.; Anderson, G. A.; Nizkorodov, S. A.; Bones, D. L.; Nguyen, L. Q. High-Resolution desorption electrospray ionization mass spectrometry for chemical characterization of organic aerosols. *Anal. Chem.* **2010**, *82* (5), 2048−2058.
(49) Roach, P. J.; Laskin, J.; Laskin, A. Molecular characterization of organic aerosols using nanospray-desorption/electrospray ionization−mass spectrometry. *Anal. Chem.* **2010**, *82* (19), 7979−7986.
(50) Kuster, W. C.; Goldan, P. D. Quantitation of the losses of gaseous sulfur compounds to enclosure walls. *Environ. Sci. Technol.* **1987**, *21* (8), 810−15.
(51) Tao, S.; Lu, X.; Levac, N.; Bateman, A. P.; Nguyen, T. B.; Bones, D. L.; Nizkorodov, S. A.; Laskin, J.; Laskin, A.; Yang, X. Molecular characterization of organosulfates in organic aerosols from Shanghai and Los Angeles urban areas by nanospray-desorption electrospray ionization high-resolution mass spectrometry. *Environ. Sci. Technol.* **2014**, *48* (18), 10993−11001.
(52) Koch, B. P.; Dittmar, T. From mass to structure: an aromaticity index for high-resolution mass data of natural organic matter. *Rapid Commun. Mass Spectrom.* **2006**, *20* (5), 926−932.
(53) Koch, B. P.; Dittmar, T. From mass to structure: an aromaticity index for high-resolution mass data of natural organic matter. *Rapid Commun. Mass Spectrom.* **2016**, *30* (1), 250−250.
(54) Lin, P.; Yu, J. Z.; Engling, G.; Kalberer, M. Organosulfates in humic-like substance fraction isolated from aerosols at seven locations in East Asia: A study by ultra-high-resolution mass spectrometry. *Environ. Sci. Technol.* **2012**, *46* (24), 13118−13127.
(55) Nguyen, Q. T.; Christensen, M. K.; Cozzi, F.; Zare, A.; Hansen, A. M. K.; Kristensen, K.; Tulinius, T. E.; Madsen, H. H.; Christensen, J. H.; Brandt, J.; Massling, A.; NÃjgaard, J. K.; Glasius, M. Understanding the anthropogenic influence on formation of biogenic secondary organic aerosols in Denmark via analysis of organosulfates and related oxidation products. *Atmos. Chem. Phys.* **2014**, *14* (17), 8961−8981.
(56) Boris, A. J.; Lee, T.; Park, T.; Choi, J.; Seo, S. J.; Collett, J. L., Jr Fog composition at Baengnyeong Island in the eastern Yellow Sea: Detecting markers of aqueous atmospheric oxidations. *Atmos. Chem. Phys.* **2016**, *16* (2), 437−453.
(57) Liggio, J.; Li, S.-M.; McLaren, R. Heterogeneous reactions of glyoxal on particulate matter: Identification of acetals and sulfate esters. *Environ. Sci. Technol.* **2005**, *39* (6), 1532−1541.
(58) Wang, X. K.; Rossignol, S.; Ma, Y.; Yao, L.; Wang, M. Y.; Chen, J. M.; George, C.; Wang, L. Molecular characterization of atmospheric particulate organosulfates in three megacities at the middle and lower reaches of the Yangtze River. *Atmos. Chem. Phys.* **2016**, *16* (4), 2285−2298.

DOI: 10.1021/acs.est.6b03304
Environ. Sci. Technol. 2017, 51, 119−127